

Molecular Characterization of NLP Function in *Nicotiana benthamiana*

Eu-Ree Ahn · Sujon Sarowar · Young Jeon · Hyun-Sook Pai

Received: 2 December 2010 / Revised: 4 February 2011 / Accepted: 7 February 2011 / Published online: 24 February 2011
© The Botanical Society of Korea 2011

Abstract In this study, we investigated the cellular functions of nuclear localizing protein (NLP) in *Nicotiana benthamiana*. The GFP fusion protein of *Arabidopsis* NLP is mostly targeted to the nucleus and cytosol, but it infrequently targets only the nucleus. Silencing of *NLP* using virus-induced gene silencing caused growth retardation and abnormal leaf development in *N. benthamiana*. At the cellular level, downregulation of *NLP* expression increased the size of pavement cells and stomata in the leaf tissues. *NLP* suppression also increased endoreduplication in leaf cells, suggesting a role of NLP in the endocycle. *NLP* transcript levels in leaves were significantly increased in response to infection with the nonhost pathogens. NLP deficiency attenuated HR cell death against nonhost pathogens and in response to gene-for-gene interaction. These findings suggest that NLP plays a role in plant development and plant defense responses against pathogens.

Keywords Endoreduplication · Increased cell size · Nuclear and cytosolic localization · Pathogen response · Virus-induced gene silencing

Eu-Ree Ahn and Sujon Sarowar contributed equally to this work

E.-R. Ahn
National Cancer Center,
Goyang-si,
Gyeonggi-do 410–769, South Korea

S. Sarowar
Department of Biological Sciences, University of North Texas,
Denton, TX, USA

E.-R. Ahn · S. Sarowar · Y. Jeon · H.-S. Pai (✉)
Department of Biology, Yonsei University,
Seoul 120–749, South Korea
e-mail: hspai@yonsei.ac.kr

Introduction

Endoreduplication is widespread in plants and often occurs in cell types that undergo specialized differentiation, such as hair cells and xylem cells, or in cell types that have high metabolic activity, such as endosperm (Joubès and Chevalier 2000; Sugimoto-Shirasu and Roberts 2003; Park et al. 2005; Inzé and De Veylder 2006; Francis 2007). Endoreduplication occurs when cells re-replicate chromosomes while mitosis is inhibited. The endocycle appears to use the same regulatory mechanism that is required for the G₁–S transition during the mitotic cell cycle (Gutierrez et al. 2002; Oakenfull et al. 2002). A role for cyclin-dependent kinases (CDKs) in endoreduplication has been demonstrated by overexpression of CDK inhibitors KIP-related proteins, which reduces endoreduplication (Schnittger et al. 2003). In contrast, overexpression of E2F transcription factors that upregulate key S-phase initiation genes elevates endoreduplication levels, indicating that the CDK-activated E2F pathway promotes S-phase entry and endoreduplication (De Veylder et al. 2002). Endoreduplication is also tightly linked with cell fate specification in *Arabidopsis* trichomes, which is regulated by specific transcription factors including *GLABRA1*, *GL3*, *TRITYCHON*, and *TRANSPARENT TESTA-GLABRA* (Sugimoto-Shirasu and Roberts 2003).

Microarray analyses revealed that transcriptional reprogramming is a key step of plant defense reactions in response to pathogen infection (Eulgem 2005). Up to 25% of *Arabidopsis* genes alter their transcript levels in response to pathogen infection, and hundreds of genes in addition to pathogenesis-related (*PR*) genes exhibit differential expression after activation of the defense program (Maleck et al. 2000; Tao et al. 2003). Recent studies on the defense transcriptome demonstrated that the signal transduction pathways of different defense systems target largely over-

lapping sets of genes. Furthermore, it has been shown that the defense transcriptome is controlled by quantitative mechanisms (Maleck et al. 2000; Tao et al. 2003; Beckers and Spoel 2006). Depending on the input signal, defense genes respond with differential timing and amplitudes, and a complex interplay between transcription activators and repressors appear to fine-tune the transcript levels of defense-associated genes (Maleck et al. 2000; Tao et al. 2003; Beckers and Spoel 2006). Interpretation of quantitative signals may be achieved by cooperative interactions of transcription factors on the promoter due to specific architecture of its *cis*-elements. Transcription factor families regulating defense genes include ERF, NPR1, R2R3 Myb, TGA bZIP, Whirly, and WRKY, but specific relationships between individual members of these families and identity of their target promoters are not well characterized (Eulgem 2005).

We attempted to address the cellular function of nuclear localizing protein (NLP) by generating a reduced-expression mutant of *NLP* by using virus-induced gene silencing (VIGS) in *Nicotiana benthamiana*. VIGS of *NLP* significantly affected plant growth and development. Furthermore, NLP deficiency also weakened plant defense responses against diverse pathogens and stimuli. Possible functions of NLP are discussed based on these phenotypes.

Materials and Methods

VIGS

The *NLP* cDNA fragments were polymerase chain reaction (PCR)-amplified and cloned into the pTV00 vector that contains a portion of the tobacco rattle virus (TRV) genome. VIGS was performed as described previously (Ahn et al. 2004; Ahn et al. 2006; Kim et al. 2006; Lee et al. 2009).

Semiquantitative Reverse Transcription-PCR

Semiquantitative reverse transcription (RT)-PCR was performed with RNA isolated from the fourth leaf above the infiltrated leaf as described previously (Kim et al. 2003; Jiang et al. 2010; Lee and Kim 2010). In total, 15–35 cycles of PCR were performed. The appropriate number of cycles was determined empirically for each template-primer pair so that amplification was in the exponential range before reaching a plateau. The endogenous *NLP* transcript was detected using the primers 5'-catcagttacagtcgc-3' and 5'-gatcaacctagaa gc-3'. To detect *PR1a*, the primers were designed on the basis of the published *N. benthamiana* cDNA sequences as described previously (Kim et al. 2003; 2006).

Flow Cytometry

Nuclei were isolated from three spots of the fourth leaf above the infiltrated leaf and stained with DAPI for flow cytometry according to the manufacturer's instructions (Partec, Germany). DNA contents of approximately 15,000 nuclei from each VIGS line were analyzed by using a PASIII flow cytometer (Partec, Germany).

Measurement of Cell Size

Leaf areas were measured using the analySIS LS research program (Olympus).

Agrobacterium-Mediated Transient Expression

Agrobacterium strain GV2260 (OD₆₀₀=0.6) containing *Pto*, *AvrPto*, *Bax*, and *INF1* were infiltrated into TRV and TRV/*NLP* lines 10 days after infection (DAI) as described previously (He et al. 2004).

Inoculation of Nonhost Pathogens

Tomato speck disease pathogen *Pseudomonas syringae* pv. *tomato* strain T1 (*PstT1*) was grown in King's B medium at 28°C. *PstT1* was infiltrated into the leaves of the VIGS lines (10 DAI) as described previously (Sarowar et al. 2007). HR cell death was visually documented at 24 h after inoculation. The pepper bacterial spot pathogen *Xanthomonas axonopodis* pv. *vesicatoria* (*Xav*) was grown in YPD medium at 30°C for infiltration. HR was visually documented 48 h after inoculation.

H₂O₂ Detection by DAB Staining

To visualize H₂O₂ in the pathogen inoculation site, 3,3'-diaminobenzidine (DAB) staining was performed as described previously (Fester and Hause 2005).

Results and Discussion

Identification of *NLP*

We have performed functional genomics using TRV-based VIGS in *N. benthamiana* (Ahn et al. 2004; 2006; Kim et al. 2006; Lee et al. 2009). The VIGS screening revealed that silencing of *NLP* caused growth retardation and abnormal leaf development. *NLP* (GenBank accession number HQ023242) encodes a 430-amino acid polypeptide with a theoretical molecular mass of 47,339.08 Da. The amino acid sequence of *NLP* was aligned with related sequences from *Arabidopsis thaliana* (*NLP*-At; At1g48580) and

Solanum tuberosum (NLP-St; TIGR gene index TC195396) (Fig. 1). These NLP homologs contain a conserved N-terminal domain and a more variable C-terminal domain. *Arabidopsis* NLP transcripts were found in all *Arabidopsis* tissues tested, with the highest level in developing and germinating seeds according to the Genvestigator program (<https://www.genevestigator.com/>).

Targeting of NLP to the Nucleus

The NLP protein was predicted to be a nuclear protein by the ESLPred algorithm (<http://www.imtech.res.in/raghava/eslpred/>). To investigate the subcellular localization of NLP, we generated a fusion protein, NLP-At:GFP, in which the full-length NLP protein of *Arabidopsis* was fused to green fluorescent protein (GFP) under the control of the CaMV35S promoter (Fig. 2). DNA constructs encoding the different GFP fusion proteins were introduced into protoplasts isolated from *Arabidopsis* seed-

lings, and after 24 h, gene expression was analyzed by fluorescent microscopy. The signal of NLP-At:GFP was mainly detected in the nucleus and cytosol, but it was infrequently detected only in the nucleus (Fig. 2a). Nuclear localization of NLP-At:GFP was confirmed by DAPI staining (Fig. 2b).

The ATTED II algorithm (http://atted.jp/top_search.shtml) predicted that the function of *Arabidopsis* NLP is most closely related to those of the transcriptional coactivator KIWI (At5g09250) and a nuclear protein of unknown function (At3g56870). KIWI was identified as an interacting protein of the PRHA transcription factor containing the homeodomain-leucine zipper domain, which is involved in the regulation of *PR* genes in *Arabidopsis* (Cormack et al. 1998). It has been suggested that KIWI is involved in signal transduction from transcription activators to the general transcription initiation factors associated with RNA polymerase for *PR* gene expression (Cormack et al. 1998). A coexpressed gene

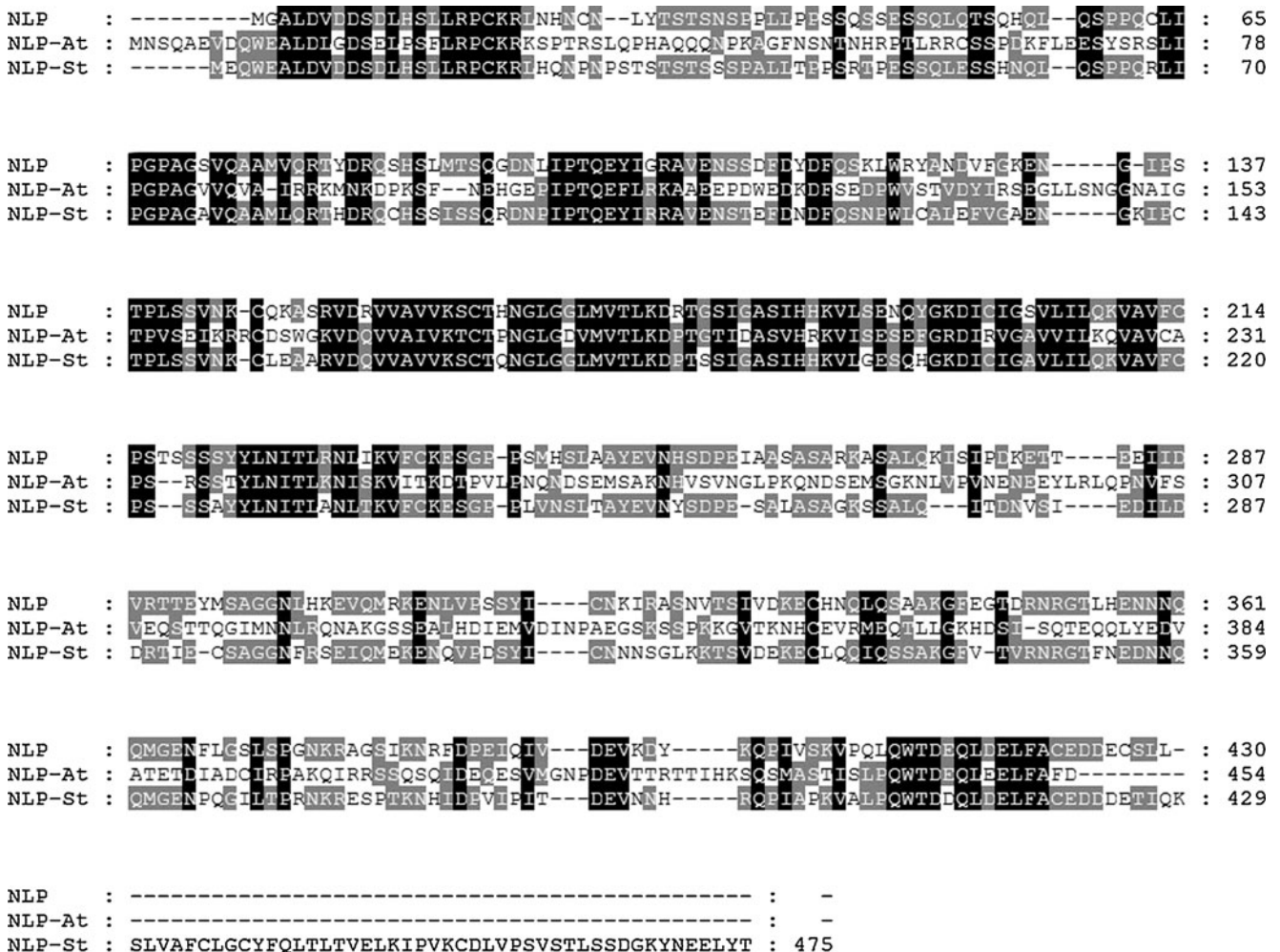


Fig. 1 Sequence alignment of NLP proteins. Amino acid sequences of NLP and its homologs from *Arabidopsis* (NLP-At) and potato (NLP-St) were aligned. The residues conserved among the compared sequences are boxed in black or light gray based on the degree of conservation

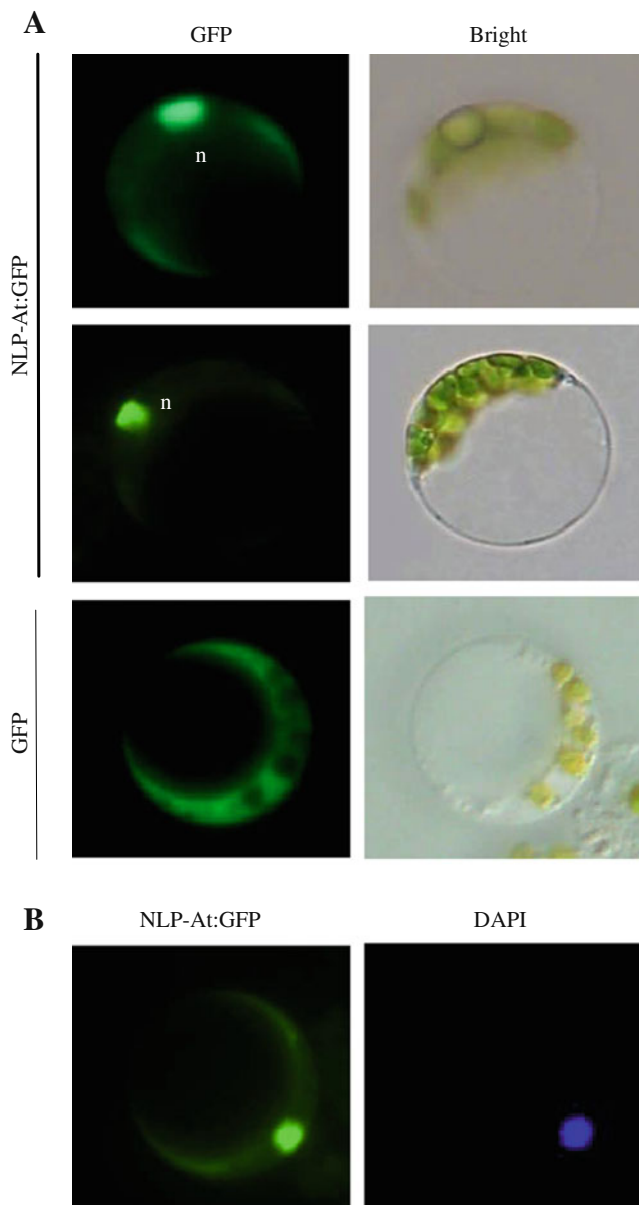


Fig. 2 Nuclear localization of NLP. **a** The subcellular localization of the NLP-At:GFP fusion protein was analyzed. *Arabidopsis* protoplasts were transformed with the fusion construct, and localization of fluorescent signals was examined 24 h after transformation by fluorescent microscopy. Fluorescence of the GFP vector control was mostly detected in the cytosol. GFP fluorescence and bright images are shown. *n*, nucleus. **b** Nuclear localization of NLP-At:GFP in the protoplasts was confirmed by DAPI staining

network search using the same algorithm also indicated that the *NLP* expression pattern is closely related to those of several transcription regulators (KIWI, BPC3 transcription factor, ANGUSTIFOLIA 3 [AN3] transcription coactivator, and TAF8 TATA-binding factor-associated factor 8) and cell cycle regulators (CDC48 and LITTLE NUCLEI2). These predictions and the nuclear localization of NLP indicate the possibility that NLP function

may be related to transcriptional regulation or cell cycle control.

VIGS of *NLP*

We cloned a 0.5-kb *NLP* cDNA fragment corresponding to the C-terminus of NLP into the TRV-based VIGS vector pTV00 and infiltrated *N. benthamiana* plants with *Agrobacterium* containing the plasmid (Fig. 3a). VIGS with this

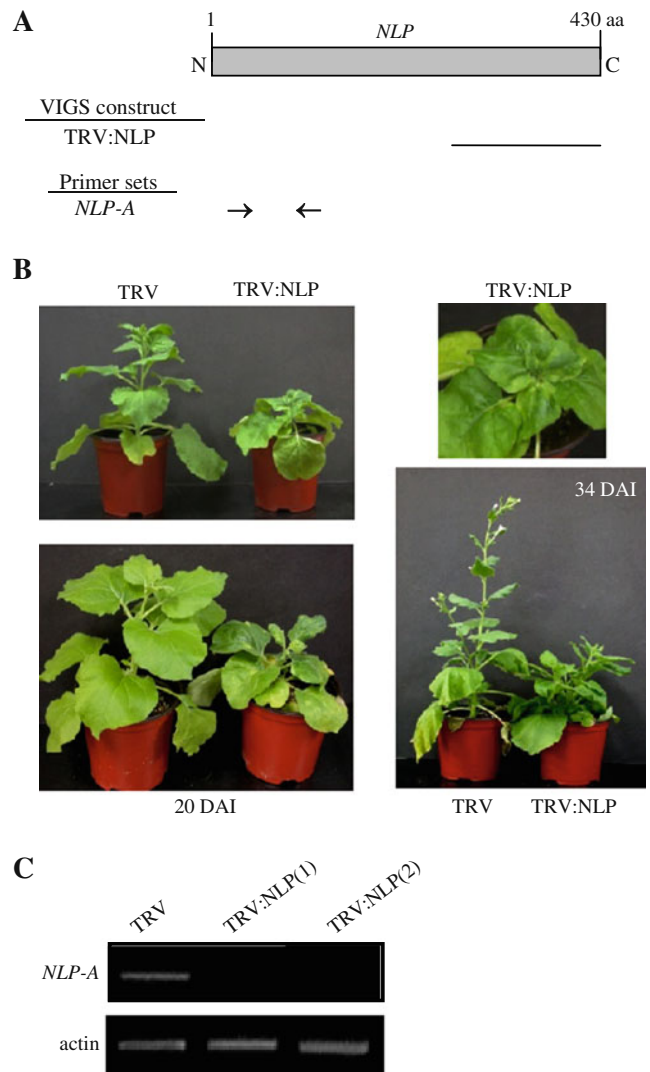


Fig. 3 VIGS phenotypes and endogenous *NLP* transcript levels. **a** Schematic representation of the *NLP* coding region and the cDNA region used in the VIGS construct. The box indicates the *NLP* protein-coding region. The VIGS construct is marked by the bar. *N. benthamiana* plants were infiltrated with *Agrobacterium* containing the TRV control or TRV/NLP construct. The position of the *NLP-A* primer sets used for semiquantitative RT-PCR analysis is indicated. aa, amino acids. **b** VIGS phenotypes. The photographs of the leaves and the whole plants were taken at 20 and 34 DAI. **c** *NLP* transcript levels were determined by semiquantitative RT-PCR. The *NLP* transcript level in two independent plants of TRV/NLP lines was compared with that of TRV control. The actin mRNA level was included as a control

construct resulted in growth retardation and abnormal leaf development (Fig. 3b). This abnormal phenotype has been observed reproducibly in all of the >70 *N. benthamiana* plants that have been subjected to *NLP* VIGS to date. The shoot apical growth was retarded, and the newly emerged leaves were irregularly shaped or wrinkled. Flower formation was also retarded in the *NLP* VIGS lines. To assess the degree of gene silencing, the amount of endogenous *NLP* mRNA in the VIGS line was determined by semiquantitative RT-PCR (Fig. 3c). RT-PCR with the *NLP-A* primers from the N-terminal region of *NLP* cDNA produced much lower levels of PCR products in two independent plants of the TRV/*NLP* line than in the TRV control plants. As a control, the transcript levels of actin remained constant (Fig. 3c). These results confirm silencing of the endogenous *NLP* in the TRV/*NLP* plants.

Increased Epidermal Cell Size in TRV/*NLP* Lines

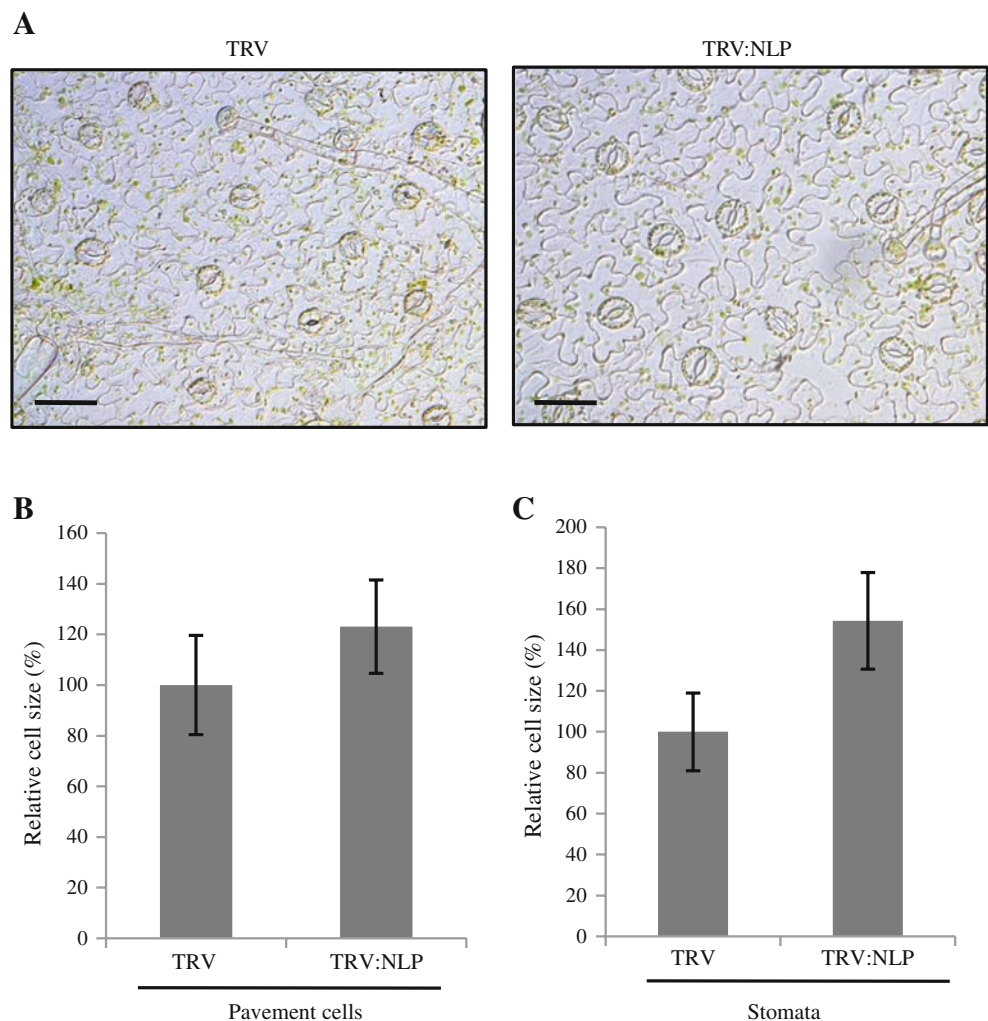
The leaf epidermal cells were observed by light microscopy (Fig. 4a). The epidermal cells of TRV controls differenti-

ated into puzzle-shaped pavement cells and stomata. TRV/*NLP* lines exhibited no gross morphological abnormalities in the leaf epidermis, but the size of pavement cells and stomata was larger than that of TRV. The average areas of the pavement cells and the stomata in TRV/*NLP* were approximately 25% and 60% larger than those of the TRV control, respectively (Fig. 4b, c).

Enhanced Endoreduplication in Leaf Cells of TRV/*NLP* Lines

Endoreduplication occurs only after the cessation of normal mitotic cycles and thus is a marker for the differentiated state of cells (Joubès and Chevalier 2000; Sugimoto-Shirasu and Roberts 2003). During endoreduplication, cells replicate chromosomal DNA without mitosis, resulting in nuclei with higher ploidy, and the resulting larger, higher ploidy nuclei are often associated with an increase in cell size (Joubès and Chevalier 2000; Sugimoto-Shirasu and Roberts 2003). As the cell size of TRV/*NLP* VIGS leaves increased compared with that of TRV control leaves, we

Fig. 4 Increased size of epidermal cells in TRV/*NLP* lines. **a** The abaxial leaf epidermis in TRV control and TRV/*NLP* lines was observed by light microscopy. The fourth leaf above the infiltrated leaf was used. Scale bars=30 μm. **b** Sizes of the pavement cells and stomata in the abaxial leaf epidermis of the TRV/*NLP* lines were measured relative to the cell size in TRV control plants. Data are expressed as mean±SD of approximately 200 individual cells



measured the ploidy levels of the nuclei isolated from three spots on TRV and TRV/NLP leaves via flow cytometry (Fig. 5a). Quantification revealed that almost all nuclei from the three spots on TRV control leaves had a ploidy level of 2C (Fig. 5b), consistent with previous reports on *N. benthamiana* and *N. tabacum* (Kosugi and Ohashi 2003; Park et al. 2005). However, the TRV/NLP line exhibited significantly increased numbers of nuclei with a ploidy level of 4C in all three spots on the leaves (Fig. 5b). The increased ploidy levels in the NLP VIGS lines suggest that NLP may play a role in the regulation of the endocycle.

The positive correlation between ploidy and cell size has been documented in many plant species. Many agricultural crops that give higher yield are polyploid, which is usually linked to their increased cell sizes (Sugimoto-Shirasu and

Roberts 2003). Endoreduplication is also associated with an increase in cell size in *Arabidopsis* (Melaragno et al. 1993), but the molecular basis for this correlation remains poorly understood. Endoreduplication defects were observed in the trichomes, leaves, and roots of *Arabidopsis* loss-of-function mutants or in plants with overexpression of cell cycle control genes and transcriptional control genes (Joubès and Chevalier 2000; Sugimoto-Shirasu and Roberts 2003). Among these, increased endoreduplication in leaves was observed in the *E2Fa-DPa*-overexpressing and *cell division control 6 (CDC6)*-overexpressing transgenic *Arabidopsis* plants (Castellano et al. 2001; De Veylder et al. 2002). E2Fa and DPa are transcription factors that control the transcription of S-phase genes (De Veylder et al. 2002), and CDC6 is part of the prereplicative complex and critically

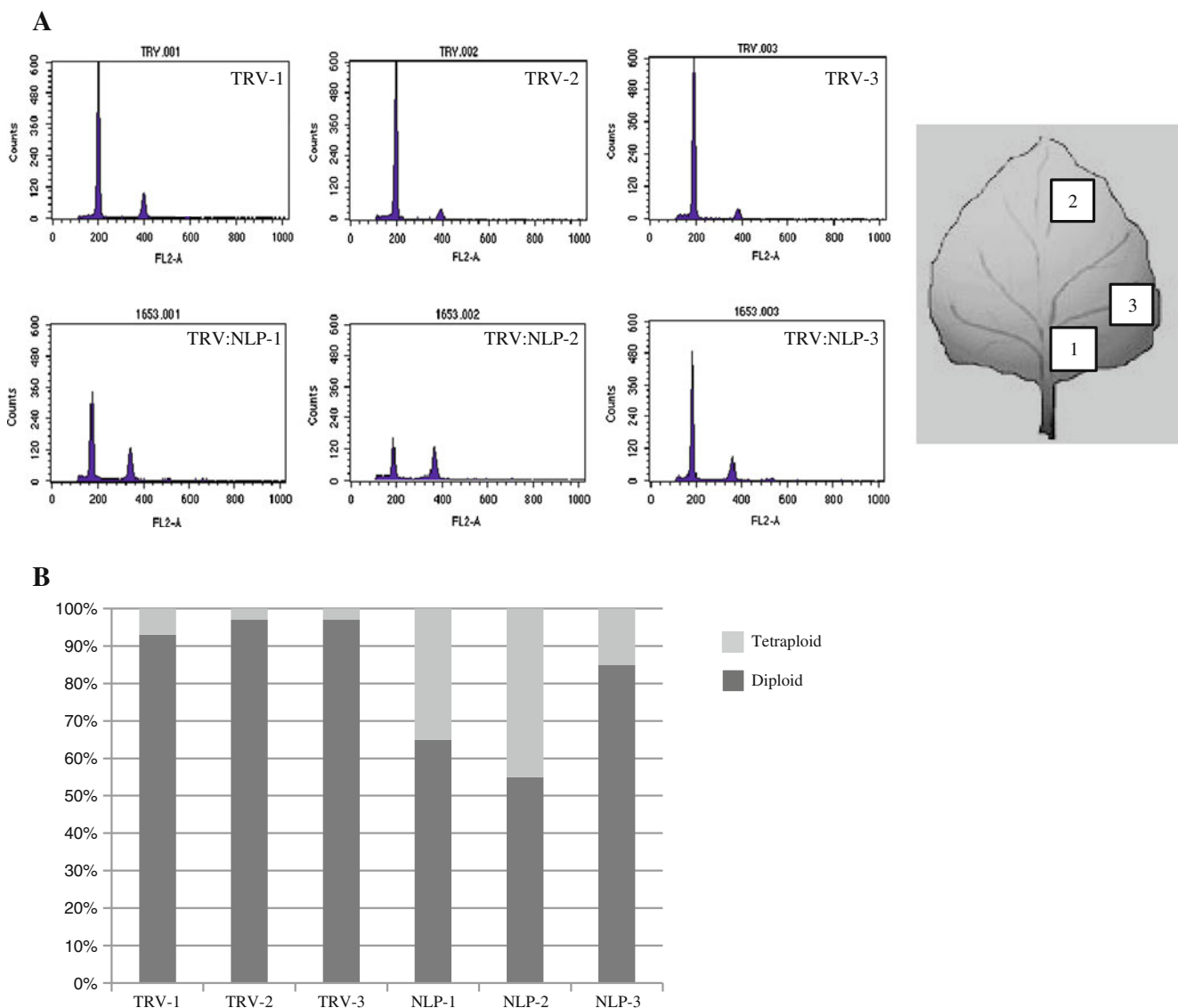


Fig. 5 DNA ploidy levels in the leaf cells of TRV and TRV/NLP lines. **a** Ploidy distribution of leaf nuclei. Approximately 15,000 nuclei isolated from three spots of the fourth leaf above the infiltrated

leaf from TRV and TRV/NLP lines were stained with DAPI and analyzed by flow cytometry. **b** Quantification of the results shown in **a**

regulates the initiation of DNA replication (Castellano et al. 2001). The *swp* mutation in *STRUWELPETER* encoding an RNA polymerase II mediator also resulted in large leaf cells and increased ploidy levels in leaves (Autran et al. 2002). Although its molecular mechanism remains unclear, increased endoreduplication in the *NLP* VIGS leaves suggest that some *NLP*-silenced cells became activated to re-enter S phase without a mitosis-inducing factor, resulting in increased ploidy levels.

Attenuation of Basal Defense Against Nonhost Pathogens in TRV/*NLP* Lines

Accumulation of *Arabidopsis NLP* transcripts significantly increased upon pathogen infection according to the Genevestigator program (<https://www.genevestigator.com/>). We examined changes of *N. benthamiana NLP* transcript levels in response to pathogen infection by semiquantitative RT-PCR (Fig. 6a). The *NLP* transcript level in leaves increased highly in response to infection of the nonhost pathogen

Pseudomonas syringae pv. *tomato* T₁ (*PstT1*), whereas the level increased moderately following infection by another nonhost pathogen, *Xanthomonas axonopodis* pv. *vesicatoria* (*Xav*). Control treatment with 10 mM MgCl₂ did not affect *NLP* expression (Fig. 6a). As a control for pathogen infection, *PR1a* transcript levels increased approximately 12 h after infection by *PstT1* and *Xav* (Fig. 6a). Because *NLP* expression was induced by nonhost pathogen infection, we tested whether *NLP* deficiency affects plant defense responses against nonhost pathogens (Fig. 6b). Leaves of TRV and TRV/*NLP* plants at 10 DAI were infiltrated with *PstT1* and *Xav* (Fig. 6b, c). In TRV control plants, *PstT1*-mediated HR cell death was detected at the pathogen concentration OD₆₀₀=0.1 and OD₆₀₀=0.01 at 24 h post-inoculation (hpi). In TRV/*NLP* leaves, *PstT1*-mediated HR was reduced at the titer OD₆₀₀=0.1 and abolished at the lower concentration (OD₆₀₀=0.01). We examined H₂O₂ production by DAB staining (Fig. 6b). H₂O₂ plays a central role in eliciting cell death and activating defense-signaling pathways. In TRV control

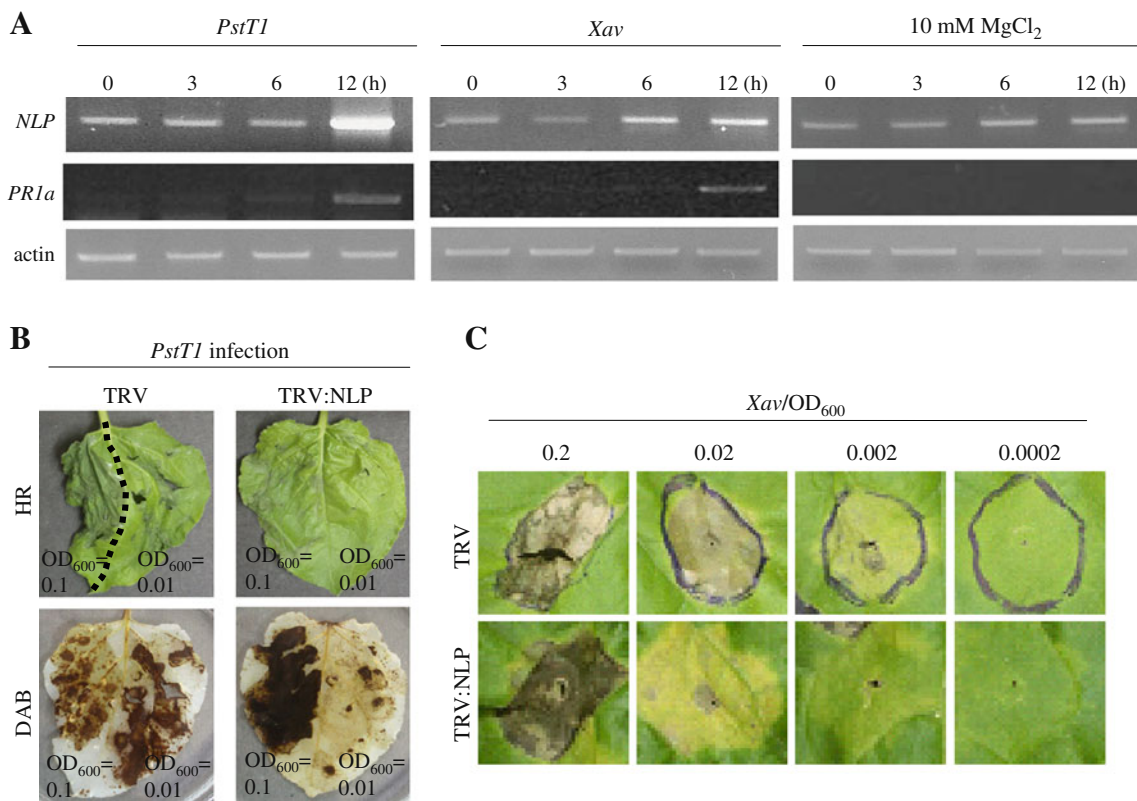


Fig. 6 Attenuation of basal defense against nonhost pathogens. **a** Semiquantitative RT-PCR for transcript levels of *NLP* in response to infection of nonhost pathogens *PstT1* and *Xav*. Plants were treated with 10 mM MgCl₂ as a negative control. As a control for pathogen infection and RNA amounts, *PR1a* and actin mRNA levels were examined. **b** HR cell death phenotypes and H₂O₂ production (DAB staining) in response to infection of *PstT1*. The fourth/fifth leaf above the infiltrated leaf of TRV and TRV/*NLP* lines (at 10 DAI) was

inoculated with *PstT1* at two different concentrations (OD₆₀₀=0.1 or 0.01). Photographs were taken at 24 hpi. The experiment was repeated three times with similar results. **c** HR phenotypes in response to infection of *Xav*. The fourth/fifth leaf above the infiltrated leaf of TRV and TRV/*NLP* lines (at 10 DAI) was inoculated with *Xav* at different concentrations. Photographs were taken at 48 hpi. The experiment was repeated three times with similar results

leaves, strong H_2O_2 staining was observed upon *PstT1* inoculation at the pathogen concentrations $OD_{600}=0.1$ and $OD_{600}=0.01$, consistent with the cell death symptoms at each titer. However, TRV/NLP leaves exhibited substantially reduced H_2O_2 staining at the titer $OD_{600}=0.01$ compared with the staining in TRV at the same titer (Fig. 6b). These results suggest that the reduced nonhost resistance against *PstT1* in TRV/NLP lines is correlated with reduced H_2O_2 production. *Xav* inoculation at the concentration of $OD_{600}=0.2$, 0.02, or 0.002 elicited HR cell death in TRV control leaves at 48 hpi, whereas inoculation at a lower concentration ($OD_{600}=0.0002$) had no effects (Fig. 6c). In contrast, HR development was significantly reduced in TRV/NLP lines at the *Xav* concentration of $OD_{600}=0.02$ or 0.002. These results indicated that HR and nonhost disease resistance were compromised in NLP-deficient plants.

Attenuation of HR Triggered by Gene-for-Gene Interaction in TRV/NLP Lines

To assess whether NLP deficiency affects HR cell death triggered by gene-for-gene interactions, we expressed *Pto*,

its cognate *avr* gene *avrPto*, or *Pto* and *avrPto* together (*Pto+avrPto*) in TRV and TRV/NLP VIGS lines by agroinfiltration (Fig. 7). In addition, *Bax* and *INF1* were also expressed in the VIGS lines. *Bax* is a mouse proapoptotic gene that triggers programmed cell death in plants (Lacomme and Santa Cruz 1999). *INF1* encodes a secreted protein of *Phytophthora infestans*, which is a known elicitor of HR in *N. benthamiana* (Kamoun et al. 1997). No HR was observed upon *Pto* expression in both TRV and TRV/NLP plants at 72 hpi (Fig. 7a, b). However, the expression of *Pto/avrPto*, *Bax*, or *INF1* induced HR in TRV leaves at 72 hpi. Expression of *avrPto* in TRV leaves induced HR cell death due to the presence of a weak endogenous *Pto*-like activity in *N. benthamiana* (He et al. 2004) (Fig. 7a, b). The frequency of HR development upon the expression of *avrPto*, *Pto/avrPto*, *Bax* or *INF1* was significantly reduced in NLP-silenced leaves compared with that in TRV control leaves (Fig. 7a, b). Particularly, NLP deficiency completely abolished HR induction by *INF1* expression. These results suggest that silencing of *NLP* attenuated HR induction in response to the *Pto/avrPto* interaction and to proapoptotic factors such as *Bax* and *INF1*. Taken together, *NLP*-silenced plants exhibited signif-

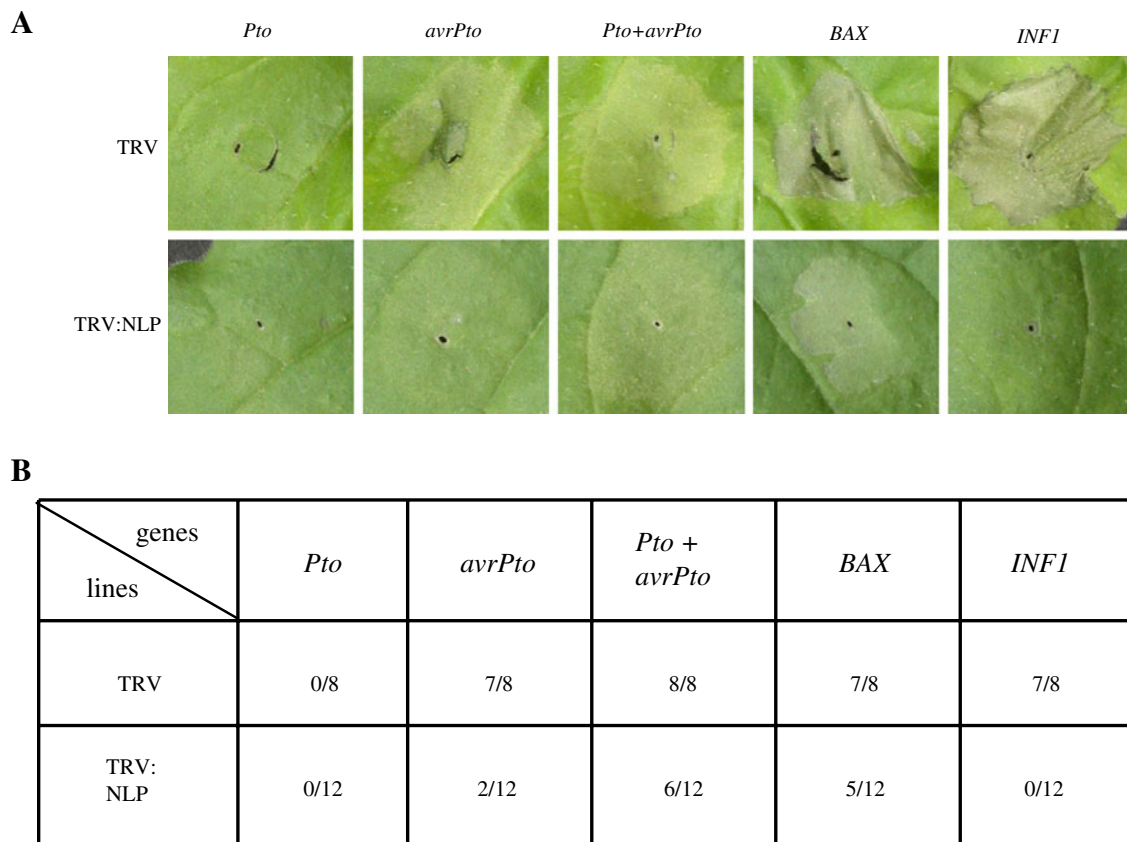


Fig. 7 Attenuation of HR triggered by gene-for-gene interactions. **a** HR cell death phenotypes after the expression of *Pto*, *AvrPto*, *Pto+AvrPto*, *Bax*, and *INF1* in TRV and TRV/NLP lines. Photographs were

taken at 72 hpi. **b** Frequency of HR induction in TRV and TRV/NLP lines after the expression of *Pto*, *AvrPto*, *Pto+AvrPto*, *Bax*, and *INF1* at 4 dpi

icantly compromised HR-inducing activity in response to nonhost pathogens and gene-for-gene interactions, suggesting that NLP contribute to multiple forms of defense response against pathogens.

As described above, the *NLP* VIGS plants exhibited delayed timing of cell death responses associated with resistance, indicating that either initial perception or subsequent signaling processes leading to cell death were impaired. Considering that NLP is localized in the nucleus and is coexpressed with the transcriptional coactivator KIWI involved in PR gene transcription through an interaction with PRHA, the impaired defense response may be caused by defects in transcriptional control upon pathogen infection. Based on our finding that NLP deficiency affects both cell growth and defense response, it is tempting to speculate that NLP may be a component of multiple transcription complexes, regulating transcriptional activation of diverse genes. Alternatively, NLP may be a nuclear component of signaling complexes that link developmental/defense signals to activation of gene expression. One example of a plant gene that has dual functions in plant development and defense is *constitutive pathogen response 5 (CPR5)*; Kirik et al. 2001). The *cpr5* mutant in *Arabidopsis* exhibited spontaneous HR cell death in the absence of pathogens, suggesting a role for CPR5 in programmed cell death control. The analysis of the *cpr5* mutants revealed an additional role for CPR5 in the regulation of endoreduplication and cell division (Kirik et al. 2001). *CPR5* encodes a putative transmembrane protein with a cytosolic domain containing a nuclear-targeting sequence. In this study, the dual role of NLP in endoreduplication and defense control suggests a regulatory link between these two processes. Deciphering the molecular networks of NLP interaction is essential for understanding the mechanism of NLP function in the control of plant growth and defense reactions.

Acknowledgments This research was supported by Mid-career Researcher Program (No. 20100026168 and No. 20100000314) and Plant Signaling Network Research Center (No. 2010–0001462), both of which are funded by National Research Foundation of Korea.

References

- Ahn J-W, Kim MI, Lim JH, Kim G-T, Pai H-S (2004) Phytoalexin controls the proliferation and differentiation fates of cells in plant organ development. *Plant J* 38:969–981
- Ahn CS, Lee JH, Hwang AR, Kim WT, Pai H-S (2006) Prohibitin is involved in mitochondrial biogenesis in plants. *Plant J* 46:658–667
- Autran D, Jonak C, Belcram K, Beecher GT, Kronenberger J, Grandjean O, Inzé D, Traas J (2002) Cell numbers and leaf development in *Arabidopsis*: a functional analysis of the *STRUWELPETER* gene. *EMBO J* 21:6036–6049
- Beckers GJ, Spoel SH (2006) Fine-tuning plant defence signalling: salicylate versus jasmonate. *Plant Biol (Stuttg)* 8:1–10
- Castellano MM, del Pozo JC, Ramirez-Parra E, Brown S, Gutierrez C (2001) Expression and stability of *Arabidopsis* CDC6 are associated with endoreplication. *Plant Cell* 13:2671–2686
- Cormack RS, Hahlbrock K, Somssich IE (1998) Isolation of putative plant transcriptional coactivators using a modified two-hybrid system incorporating a GFP reporter gene. *Plant J* 14:685–692
- De Veylder L, Beeckman T, Beecher GTS, Engler JDA, Ormenese S, Maes S, Naudts M, Schueren EVD, Jacquard A, Engler G, Inzé D (2002) Control of proliferation, endoreduplication and differentiation by the *Arabidopsis* E2Fa-DPa transcription factor. *EMBO J* 21:1360–1368
- Eulgem T (2005) Regulation of the *Arabidopsis* defense transcriptome. *Trends Plant Sci* 10:71–78
- Fester T, Hause G (2005) Accumulation of reactive oxygen species in arbuscular mycorrhizal roots. *Mycorrhiza* 15:373–379
- Francis D (2007) The plant cell cycle—15 years on. *New Phytol* 174:261–278
- Gutierrez C, Ramirez-Parra E, Castellano MM, del Pozo JC (2002) G (1) to S transition: more than a cell cycle engine switch. *Curr Opin Plant Biol* 5:480–486
- He X, Anderson JC, del Pozo O, Gu Y-Q, Tang X, Martin GB (2004) Silencing of subfamily I of protein phosphatase 2A catalytic subunits results in inactivation of plant defense responses and localized cell death. *Plant J* 38:563–577
- Inzé D, De Veylder L (2006) Cell cycle regulation in plant development. *Annu Rev Genet* 40:77–105
- Jiang W, Fu F-L, Zhang S-Z, Wu L, Li W-C (2010) Cloning and characterization of functional trehalose-6-phosphate synthase gene in maize. *J Plant Biol* 53:134–141
- Joubès J, Chevalier C (2000) Endoreduplication in higher plants. *Plant Mol Biol* 43:735–745
- Kamoun S, van West P, de Jong AJ, de Groot KE, Vleeshouwers VG, Govers F (1997) A gene encoding a protein elicitor of *Phytophthora infestans* is down-regulated during infection of potato. *Mol Plant-Microb Interact* 10:13–20
- Kim MI, Ahn J-W, Jin U-H, Paek K-H, Pai H-S (2003) Activation of the programmed cell death pathway by inhibition of proteasome function in plants. *J Biol Chem* 278:19406–19415
- Kim M, Lim J-H, Ahn CS, Park K, Kim GT, Kim WT, Pai H-S (2006) Mitochondria-associated hexokinases play a role in the control of programmed cell death in *Nicotiana benthamiana*. *Plant Cell* 18:2341–2355
- Kirik V, Bouyer D, Schöbinger U, Bechtold N, Herzog M, Bonneville JM, Hülskamp M (2001) CPR5 is involved in cell proliferation and cell death control and encodes a novel transmembrane protein. *Curr Biol* 11:1891–1895
- Kosugi S, Ohashi Y (2003) Constitutive E2F expression in tobacco plants exhibits altered cell cycle control and morphological change in a cell type-specific manner. *Plant Physiol* 132:2012–2022
- Lacomme C, Santa Cruz S (1999) Bax-induced cell death in tobacco is similar to the hypersensitive response. *Proc Natl Acad Sci USA* 96:7956–7961
- Lee HW, Kim J (2010) Ectopic expression of *LBD18/ASL20* results in arrest of plant growth and development with repression of *AINTEGUMENTA* and *PLETHORA* genes. *J Plant Biol* 53:214–221
- Lee JY, Lee HS, Wi SJ, Park KY, Schmit AC, Pai H-S (2009) Dual functions of *Nicotiana benthamiana* Rael1 in interphase and mitosis. *Plant J* 59:278–291
- Maleck K, Levine A, Eulgem T, Morgan A, Schmid J, Lawton KA, Dangl JL, Dietrich RA (2000) The transcriptome of *Arabidopsis thaliana* during systemic acquired resistance. *Nat Genet* 26:403–410

- Melaragno JE, Mehrotra B, Coleman AW (1993) Relationship between endopolyploidy and cell size in epidermal tissue of *Arabidopsis*. *Plant Cell* 5:1661–1668
- Oakenfull EA, Riou-Khamlichi C, Murray JA (2002) Plant D-type cyclins and the control of G1 progression. *Philos Trans R Soc Lond B Biol Sci* 357:749–760
- Park J-A, Ahn J-W, Kim Y-K, Kim SJ, Kim J-K, Kim WT, Pai H-S (2005) Retinoblastoma protein regulates cell proliferation, differentiation, and endoreduplication in plants. *Plant J* 42:153–163
- Sarowar S, Oh HW, Cho HS, Baek KH, Seong ES, Joung YH, Choi GJ, Lee S, Choi D (2007) *Capsicum annuum* CCR4-associated factor CaCAF1 is necessary for plant development and defence response. *Plant J* 51:792–802
- Schnittger A, Weigl C, Bouyer D, Schöbinger U, Hülskamp M (2003) Misexpression of the cyclin-dependent kinase inhibitor ICK1/KRP1 in single-celled *Arabidopsis* trichomes reduces endoreduplication and cell size and induces cell death. *Plant Cell* 15:303–315
- Sugimoto-Shirasu K, Roberts K (2003) “Big it up”: endoreduplication and cell-size control in plants. *Curr Opin Plant Biol* 6:544–553
- Tao Y, Xie Z, Chen W, Glazebrook J, Chang HS, Han B, Zhu T, Zou G, Katagiri F (2003) Quantitative nature of *Arabidopsis* responses during compatible and incompatible interactions with the bacterial pathogen *Pseudomonas syringae*. *Plant Cell* 15:317–330